PIER C

(Received 13 January 2025, Accepted 20 February 2025, Scheduled 1 March 2025)

Yagi-Antenna Array Loaded with Multi-Layer Composite Decoupling Structure

Minjie Guo*, Junkang Song, Xiaohei Yan, Haiyan Zeng, Xin Zheng, Xiumei Huang, and Shanglin Xie

School of Physics and Electric Information Engineering, Guangxi Minzu Normal University, Chongzuo 532200, Guangxi, China

ABSTRACT: In this paper, a multi-layer decoupling metamaterial unit (ML-DMU) is proposed to reduce the mutual coupling in a Yagi-antenna array. ML-DMU is a three-layer structure which is composed of two types of decoupling unit named top and bottom unit, middle unit, respectively. On this basis, the $|S_{21}|$ of proposed array is reduced to less than -23 dB from 2.36 GHz to 3.02 GHz while the antenna volume is not changed. The maximum gain of antenna element in the proposed antenna is 6.56 dBi at 3 GHz, which is greater than the antenna without ML-DMU, but smaller than a single antenna element. Compared with other composite decoupling structures, the decoupling structure proposed in this paper has a more stable radiation performance and is simple and easy to install, which makes it have a good prospect in the field of 5G communication and the field of near-earth ground penetrating radar.

1. INTRODUCTION

In recent years, antenna arrays have become more and more widely used in 5G communication systems and shallow ground penetrating radar. However, owing to the mutual coupling between two adjacent antenna elements, the radiation characteristics such as antenna gain and radiation efficiency will be significantly affected. In order to reduce the influence of mutual coupling, researchers have proposed a variety of methods, such as reflection structure, parasitic decoupling structure, self-decoupling characteristic structure, defective ground structure (DGS), and metamaterial.

Reflection structure, which has a little influence on radiation pattern and antenna gain, can significantly reduce the mutual coupling between antennas. In [1], a metal block is utilized to reduce the mutual coupling in a $2 \times N$ array, and the coupling patches among the horizontal, vertical diagonal, and non-adjacent elements are suppressed to less than -27 dB. Partial reflective decoupling layers (PRDLs) presented in [2] can also increase the isolation between two antennas to more than 21 dB. In addition, by mixing with an array-antenna decoupling surface (ADS) and artificial magnetic conductor (AMC), the isolation in [3] is better than 22 dB from 3.2 to 3.8 GHz. Similarly, by using partial reflective decoupling layers (PRDLs) between two closely spaced dipole antennas, the isolation in [4] can be reduced to more than 21 dB.

By loading a parasitic shorting C-shaped structure in [5, 6], the isolation between antenna elements is enhanced significantly. Similarly, patch antenna array with a parasitic structure, which consists of a microstrip L-section array and a microstrip U-section array in [7], and the π-shaped decoupling structure presented in [8, 9] can also achieve a good decoupling effect. Fence-type decoupling structure using in [10] can reduce the mutual coupling to -25 dB in the UWB.

In addition, the self-decoupling mechanism is used in [11, 12] to reduce the mutual coupling for MIMO antennas. The DGS proposed in [13, 14] can also significantly reduce the mutual coupling.

Metamaterials have great potential to reduce the coupling between antenna arrays, and they mainly appear in the form of metasurface or absorber. By using metasurface decoupling method, the isolation between two antennas can be improved to more than 25 dB in [15–17]. At the same time, by using a dual-layer metamaterial absorber unit cell, the mutual coupling level of -65.4 dB is achieved in [18]. A double-layer metamaterial absorber wall placed in four-element antenna array can also improve the isolation in [19] to more than 8 dB. Although the proposed method has obvious effects in terms of decoupling, the decoupling structure, consisting of different decoupling units, is rarely mentioned.

In this paper, a composite decoupling structure is proposed, which is composed of two types of decoupling units. In Section 2, the design process of decoupling structure and antenna array is shown in detail. In Section 3, the simulated and measured results are compared and discussed. The conclusion is shown in Section 4.

2. ML-DMU DESIGN

The proposed ML-DMU in this paper consists of a top layer, a middle layer, and a bottom layer. The top and bottom layers have the same geometry but are placed symmetrically with the middle layer as the center.

2.1. Top and Bottom Unit Design

Figure 1(a) shows the geometry of top and bottom decoupling units which have a double-layer structure, and a spider-shaped metal patch is etched on an FR4 substrate with a thickness of

* Corresponding author: Minjie Guo (guominjie@gxnun.edu.cn).

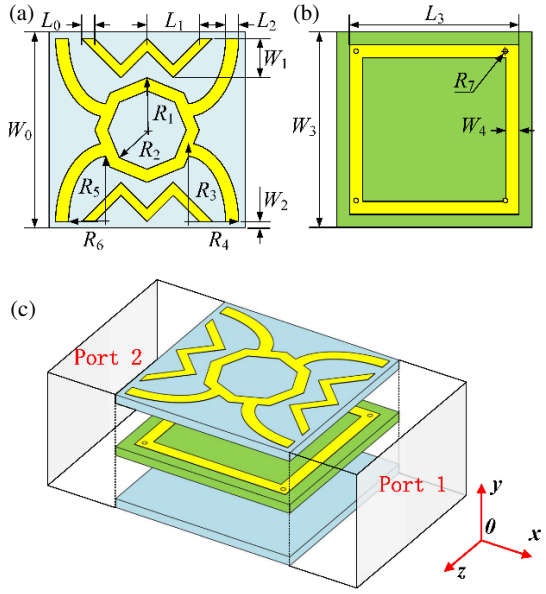

FIGURE 1. Geometries and simulation model of decoupling units.

1 mm. Same as Fig. 1(c), the simulation model adopts the "unit cell" boundary condition in the y and z directions, and the electromagnetic wave propagates along the x axis. The geometry parameters of this unit are shown in Table 1. Fig. 2 shows the magnitude of its reflection and transmission coefficient. It can be seen that the $|S_{11}|$ of top and bottom units is larger than 0.8, and the $|S_{21}|$ is lower than 0.3 in the operation frequency band, which means that most of the electromagnetic waves from the side of decoupling unit are reflected, and only a little of energy passes through the unit to the other side.

TABLE 1. Geometry parameters of proposed antenna. (Unit: mm).

L	L_0	L_1	L_2	L_3	L_4	L_5	L_6
120	1.35	5.4	1.35	20.25	20	21	24
L_7	L_8	L_9	L_{10}	W	W_0	W_1	W_2
22.775	20.25	7	4	70	20.25	4.05	0.675
W_3	W_4	W_5	W_6	W_7	W_8	W_9	W_{10}
20.25	1.35	40.5	5	6	15	3	10
W_{11}	R_1	R_2	R_3	R_4	R_5	R_6	R_7
20	5.4	4.05	8.1	5.4	6.75	4.05	0.5

2.2. Middle Unit Design

The geometry of middle unit is shown in Fig. 1(b). It consists of square metal rings located on the upper and bottom sides of the substrate and metal cylinders located at four corners. The substrate is FR4 with a thickness of 1 mm, and thickness of the metal patch here is 0.035 mm. The geometry parameters of this unit are also shown in Table 1. Minimum reflection coefficient here is 0.95 at 3.02 GHz while the maximum transmission coefficient is 0.25, and the energy from one side of the unit is difficult to cross through this structure to the other side.

2.3. ML-DMU Design

In order to further improve the decoupling effect, ML-DMU is formed by placing two top and bottom units symmetrically on both sides of a middle unit while the metal layer is placed facing outward. The geometry and simulation model of ML-DMU are shown in Fig. 1(c). The distance between the two types of units is 0 mm. The simulated S-parameter of ML-DMU is shown in Fig. 2. Similarly, ML-DMU has better reflective properties and lower transmission coefficient than the above-mentioned two units, and it will reflect most of energy from the antenna sides.

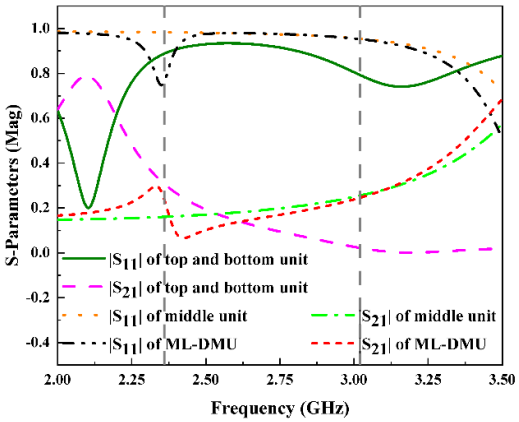

FIGURE 2. Comparison of the amplitudes of the S-parameters of the decoupling units.

Figure 3 shows the $|S_{21}|$ comparison results of the original antenna array loaded with the decoupling units composed of pure units of the top and bottom units, middle unit, and ML-DMU, respectively. Obviously, ML-DMU structure has a lower $|S_{21}|$ in Band 1 compared with the top and bottom units. At the same time, compared with the middle unit, ML-DMU structure has a much obvious resonance point in Band 2. Moreover, by adjusting the size of the square ring in the middle unit, the mutual coupling in different frequency bands can be similarly reduced. With all these reasons above, ML-DMU has a better decoupling effect than the combination of the single elements.

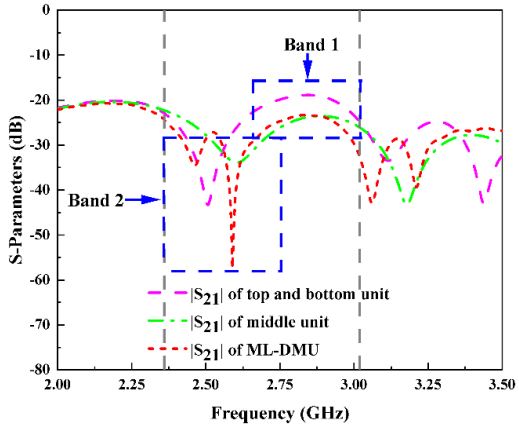

FIGURE 3. $|S_{21}|$ when loading different decoupling units.

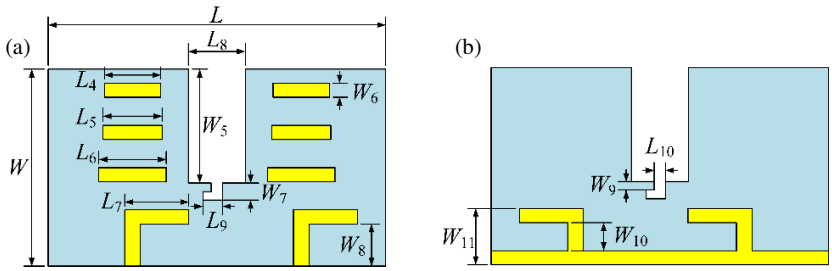

FIGURE 4. Geometry of Yagi-antenna array.

2.4. Antenna Array Design

Figure 4 illustrates the geometry of a Yagi-antenna array used in this paper. Antenna element is designed on an FR4 ($\varepsilon_r = 4.4$, $\tan\sigma = 0.025$) substrate with a thickness of 3 mm. The top layer of each antenna element consists of a feedline, a driver, and three directors. The reflector and the other driver are etched on the bottom side of the substrate. On this basis, a rectangular groove with a hook is machined in the center of the substrate to facilitate the installation of ML-DMU. Geometry parameters in Fig. 4 are shown in Table 1.

3. RESULTS COMPARISON AND DISCUSSION

At the foundation of the above analysis, the proposed antenna is fabricated and installed in Figs. 5(a)–(d). Figs. 5(e)–(g) show the test processing of antenna array with ML-DMU, and the testing process for other antennas in this paper is similar to this. The ML-DMU is transitionally fit and connected with the proposed antenna by means of an "L" shaped hook. Since the thickness of ML-DMU is slightly larger than the antenna array substrate, the upper surface of the substrate is used as the reference plane to install these structures.

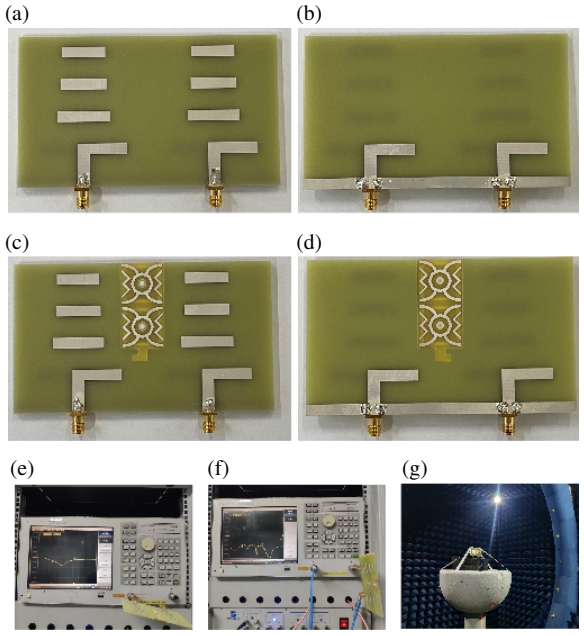

FIGURE 5. Photographs of the target antenna array and test processing.

3.1. *S*-Parameters Comparison

Figure 6 shows a comparison of the S-parameters obtained by the CST studio suite and the measured results obtained by the vector network analyzer. Operation frequency of the proposed antenna array is 2.36–3.02 GHz, which covers the frequency band of 5G communication. Compared to the antenna array, the bandwidth of target antenna is increased by 0.16 GHz. At the same time, the measured $|S_{21}|$ of the target antenna is reduced to less than -23 dB in the operation frequency band, and the maximum reduction occurs around 2.5–2.6 GHz. Due to the large step width in the testing process, there is a certain difference between the measured and simulated results, but it does not affect the use of the antenna.

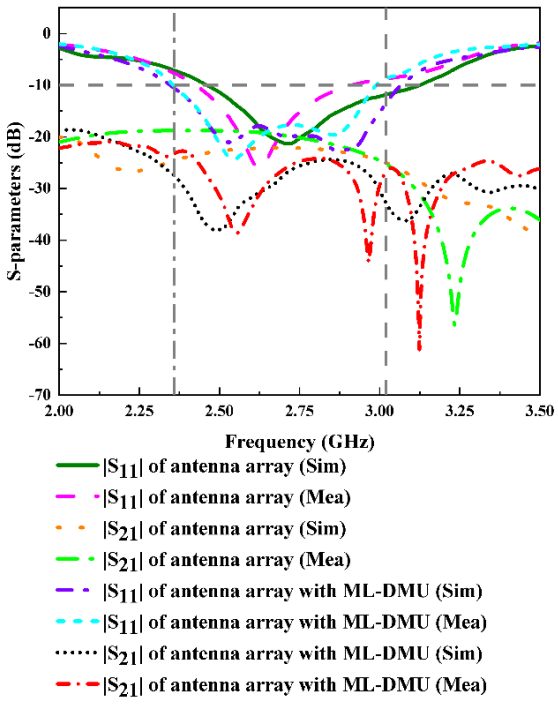

FIGURE 6. S-parameters comparison results.

3.2. Gain and Radiation Comparison

In order to analyze the radiation performance of the designed antenna, the performances of antenna element, antenna array with and without ML-DMU obtained from CST studio suite and microwave darkroom are compared in Fig. 7 and Fig. 8. As shown in Fig. 7, gain of the antenna element before and af-

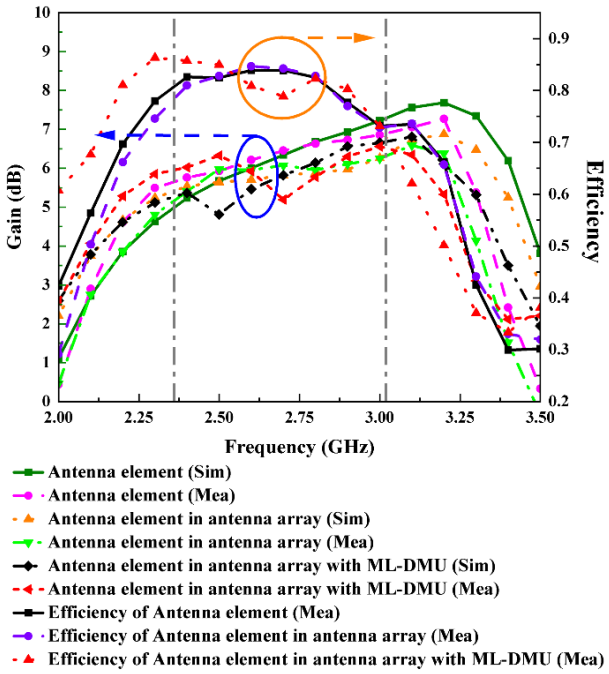

FIGURE 7. Gain and radiation efficiency comparison results.

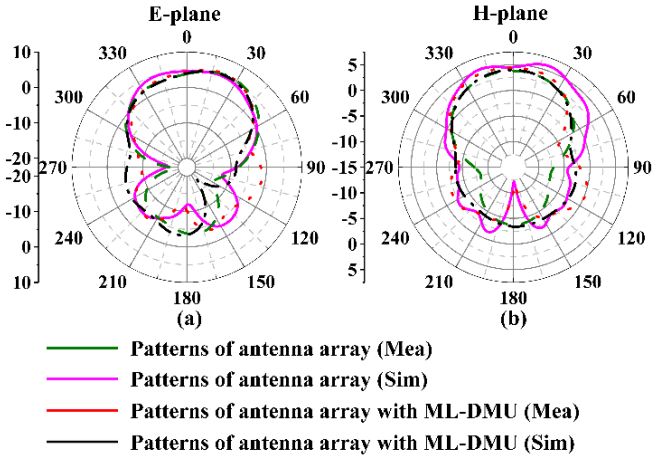

FIGURE 8. Radiation patterns with antenna gain at 2.6 GHz.

ter loading ML-DMU changes little in the operating frequency band, but due to the influence of antenna mutual coupling, the antenna gain in antenna array is reduced compared with a single antenna element, but the maximum gain reduction does not exceed 0.67 dB while the gain reduction does not exceed 0.85 dB in the proposed antenna array. In addition, the peak gain of antenna element in antenna array with ML-DMU is about 6.56 dBi at 3 GHz. Thanks to the ML-DMU, the antenna gain increases to some extent in some frequency points compared with that without one, which is different from the traditional decoupling method.

Figure 7 also shows the comparison results of radiation efficiency of antenna element before and after the array is assembled and loaded with the ML-DMU. It is evident that the antenna efficiency of antenna element decreases after loading with ML-DMU, but the minimum antenna efficiency in the operating frequency band is still greater than 73%.

Radiation patterns of target antenna array with and without ML-DMU at 2.6 GHz are depicted in Fig. 8 to study the directivity differences. It is clear that the difference between the measured and simulated results is small in the end-fire direction regardless of the E-plane or H-plane patterns. In addition, the antenna arrays with and without ML-DMU have an obviously narrower main lobe in the end-fire direction. However, the sidelobe and back lobe of the antenna patterns were enlarged and split due to the influence of the test environment and SMA connector flanges. At the same time, the main lobe levels of antenna array before and after loading ML-DMU change little, which means that the ML-DMU has little interference in antenna radiation performance.

3.3. *E*-Field Comparison

Figure 9 shows the E-field contributions at 2.6 GHz with and without ML-DMU. Obviously, the radiated energy from the side of the right antenna can be significantly reflected by the ML-DMU. The mutual coupling here is weakened, and the radiation performance of the left antenna is almost not affected.

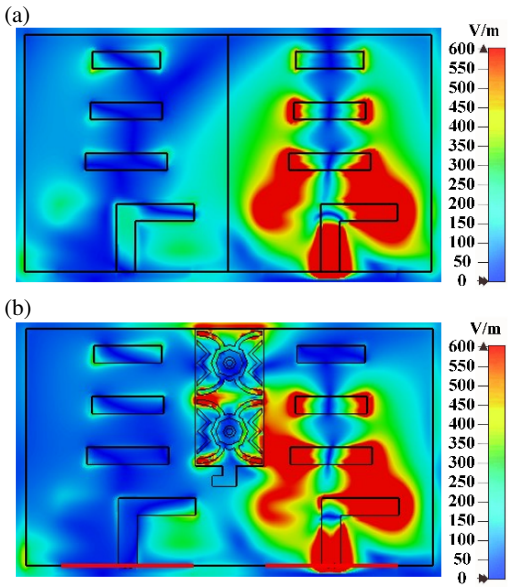

FIGURE 9. E-field comparison at 2.6 GHz.

In order to determine the advantages and disadvantages of the decoupling structure proposed in this paper, the designed structure is compared with other recently proposed decoupling structures, and the comparison results are shown in Table 2. All of the antennas listed in Table 2 operate around 1–4 GHz, where the number of antenna elements in [1] and [19] is greater than 2. Compared with [1] and [15], the proposed antenna array has a lower total efficiency, but its isolation in operation frequency is greater than [14] and [19]. At the same time, although a three-layer decoupling structure is introduced, the antenna array designed in this paper still has a smaller volume than other works in [1, 5, 15, 19].

TABLE 2. Comparison with other works.

Ref.	Mechanism	Total efficiency	Isolation (dB)	Volume (mm^3)
This paper	Multi-layer decoupling structure	$> 73\%$	> 23	$120 \times 90 \times 3.2$
[1]	Metal block	$> 79\%$	> 26.9	$\approx 342.4 \times 42.8 \times 14.8$
[5]	Parasitic decoupling structure	unknow	> 31	$140 \times 80 \times 3$
[14]	Defected ground structure	unknow	> 22	$70 \times 40 \times 3$
[15]	Meta-surface	$> 83\%$	> 25	$150 \times 150 \times 52$
[19]	Metamaterial absorber	unknow	> 22	$190 \times 190 \times 48$

4. CONCLUSION

In this paper, a three-layer decoupling unit consists of top and bottom units, middle unit is proposed to improve the isolation in a Yagi-antenna array. The two different structural units used here have reflection and absorption characteristics respectively, and the final combined ML-DMU structure has obvious energy reflection characteristics. When the ML-DMU is installed between the transmitting and receiving antennas, the $|S_{21}|$ between antenna elements can be reduced to less than -23 dB at 2.3–3.02 GHz. Moreover, the peak gain of antenna element in target array is 6.56 dBi at 3 GHz while the antenna volume is not changed. Compared to other composite decoupling structures, ML-DMU is composed of different types of units and has a certain gain enhancement effect, which makes it have a good application prospect in 5G communication and shallow ground penetrating radar.

ACKNOWLEDGEMENT

This work was supported by the Guangxi Natural Science Foundation (Grant No. 2022JJB150010), the Basic Research Ability Improvement Project for Young and Middle-aged Teachers in Guangxi Universities (Grant No. 2023KY0793), and the School-level Research Project of Guangxi Minzu Normal University (Grant No. 2022SP005).

REFERENCES

[1] Zhang, Y.-M. and S. Zhang, "A side-loaded-metal decoupling method for 2 × N patch antenna arrays," *IEEE Antennas and Wireless Propagation Letters*, Vol. 20, No. 5, 668–672, Feb. 2021.

[2] Liu, T., J. Jiang, L. Zhao, G. Zhao, H. Zhai, Y.-M. Cai, T. Chen, and W. Xu, "Compact U6G massive MIMO antenna arrays with double-layer partial reflective decoupling layers for mutual coupling suppression," *IEEE Open Journal of Antennas and Propagation*, Vol. 4, 764–778, Jul. 2023.

[3] Yuan, H. and F.-C. Chen, "A mixed decoupling scheme based on AMC and ADS for dual-polarized antenna array," *IEEE Transactions on Antennas and Propagation*, Vol. 71, No. 7, 6150–6155, Apr. 2023.

[4] Zhao, G., T. Liu, J. Jiang, L. Zhao, G.-L. Huang, and W. Lin, "Polarization selective partial reflective decoupling layers for mutual coupling reduction of two closely spaced dual-polarized antennas," *IEEE Transactions on Antennas and Propagation*, Vol. 70, No. 11, 11 205–11 210, Jul. 2022.

[5] Fang, Y., M. Tang, and Y. P. Zhang, "A decoupling structure for mutual coupling suppression in stacked microstrip patch antenna array," *IEEE Antennas and Wireless Propagation Letters*, Vol. 21, No. 6, 1110–1114, Mar. 2022.

[6] Zhang, Y. and Y. Zhang, "Dual-band dual-polarized antenna using a simple radiation restoration and decoupling structure," *IEEE Antennas and Wireless Propagation Letters*, Vol. 22, No. 4, 709–713, Nov. 2022.

[7] Xie, M., X. Wei, Y. Tang, and D. Hu, "A parasitic decoupling structure for dual-polarized patch antenna arrays," *IEEE Antennas and Wireless Propagation Letters*, Vol. 22, No. 6, 1351–1355, Feb. 2023.

[8] Su, S.-W., C.-T. Lee, and Y.-W. Hsiao, "Compact two-inverted-F-antenna system with highly integrated π-shaped decoupling structure," *IEEE Transactions on Antennas and Propagation*, Vol. 67, No. 9, 6182–6186, Jul. 2019.

[9] Yang, M., C. Liu, and X. Liu, "Design of π-shaped decoupling network for dual-polarized Y-probe antenna arrays," *IEEE Antennas and Wireless Propagation Letters*, Vol. 21, No. 6, 1129–1133, Mar. 2022.

[10] Wang, L., Z. Du, H. Yang, R. Ma, Y. Zhao, X. Cui, and X. Xi, "Compact UWB MIMO antenna with high isolation using fence-type decoupling structure," *IEEE Antennas and Wireless Propagation Letters*, Vol. 18, No. 8, 1641–1645, Jul. 2019.

[11] Yang, B., Y. Xu, J. Tong, Y. Zhang, Y. Feng, and Y. Hu, "Tri-port antenna with shared radiator and self-decoupling characteristic for 5G smartphone application," *IEEE Transactions on Antennas and Propagation*, Vol. 70, No. 6, 4836–4841, Dec. 2021.

[12] Sui, J., C. Huang, J. Li, X. Zhu, and D. Li, "Wideband aperture-overlapped MIMO antennas naturally integrating mode orthogonal and parasitic decoupling schemes," *IEEE Antennas and Wireless Propagation Letters*, Vol. 23, No. 8, 2441–2445, Apr. 2024.

[13] Qian, B., X. Chen, L. Zhao, J. Chen, and A. A. Kishk, "Reduced cross-polarization and backside radiations for rectangular microstrip antennas using defected ground structure combined with decoupling structure," *IEEE Antennas and Wireless Propagation Letters*, Vol. 22, No. 3, 517–521, Oct. 2022.

[14] Yang, Z., J. Xiao, and Q. Ye, "Enhancing MIMO antenna isolation characteristic by manipulating the propagation of surface wave," *IEEE Access*, Vol. 8, 115 572–115 581, Jun. 2020.

[15] Liu, F., J. Guo, L. Zhao, X. Shen, and Y. Yin, "A meta-surface decoupling method for two linear polarized antenna array in sub-6 GHz base station applications," *IEEE Access*, Vol. 7, 2759–2768, Dec. 2018.

[16] Liu, F., J. Guo, L. Zhao, G.-L. Huang, Y. Li, and Y. Yin, "Dual-band metasurface-based decoupling method for two closely packed dual-band antennas," *IEEE Transactions on Antennas and Propagation*, Vol. 68, No. 1, 552–557, Sep. 2019.

[17] Li, M., J. Mei, X.-X. Yang, D. Zeng, and Z. Yi, "Isolation enhancement based on metasurface for dual-band E/H-plane coupled antenna array," *IEEE Antennas and Wireless Propagation Letters*, Vol. 23, No. 7, 2234–2238, Apr. 2024.

[18] Gong, Y., R. Morawski, and T. Le-Ngoc, "Metamaterial absorber structure for Tx-Rx antenna isolation improvement in full-duplex massive MIMO," *IEEE Access*, Vol. 12, 64 571–64 588, May 2024.

[19] Zhang, J., J. Li, and J. Chen, "Mutual coupling reduction of a circularly polarized four-element antenna array using metamaterial absorber for unmanned vehicles," *IEEE Access*, Vol. 7, 57 469–57 475, Apr. 2019.